COMMUNICATION

Directing Colloidal Self-Assembly with Biaxial Electric Fields

By *Mirjam E. Leunissen,* Hanumantha Rao Vutukuri,* and *Alfons van Blaaderen**

Microscopic 'colloidal' particles can spontaneously organize into larger-scale structures, making them important as condensed-matter model systems[1] and advanced materials.[2–4] Nowadays, one can often predict what structure is needed to obtain certain material properties;[5,6] the challenge is to experimentally realize the, often complex, particle interactions that lead to those structures.[7] External fields provide one route.[8] Uniaxial electric and magnetic fields are commonly used to induce dipolar interactions,[9,10] while multi-axial fields bear promise for higher complexity of the interactions.[11,12] Here, we focus on a biaxial electric field, generated by applying a high-frequency 2D field vector with a randomized orientation, and study in detail how the resulting 'inverted' dipolar interactions affect the colloidal self-assembly process. We find that the particles reproducibly form a (most likely non-equilibrium) structure of hexagonal 'sheets', which we can make permanent by thermal annealing. Moreover, we can rapidly switch the suspension structure from isotropic, to one-dimensional 'strings' and two-dimensional 'sheets'. This is interesting for applications, because the sample spanning sheets make the suspension properties strongly anisotropic[13] and can dramatically increase the viscosity[14] and thermal conductivity.[15] While the fairly simple inverted dipolar interaction already gives structures that are rather different from those seen in uniaxial fields, our approach could easily be extended to other, more complex interaction potentials as well, by choosing different time-varying functions on the electrodes.

For decades, colloidal studies have mostly been concerned with particles with straightforward shapes and simple, mainly isotropic, interactions.[16] This sets certain bounds to their applicability as models of atomic/molecular phase behavior[1] and the number of structures that can be obtained through self-assembly. However, advances in synthesis and chemical modification have recently led to new particle shapes and interaction forms,[17–19] while external electric or magnetic fields can be used to induce new interactions in existing systems.[9,10] A major advantage of the latter approach is that the interactions are reversible and that it does not require complicated chemistry.

[*] Dr. M. E. Leunissen,[+] Prof. A. van Blaaderen, H. R. Vutukuri
Soft Condensed Matter
Debye Institute for Nanomaterials Science
Utrecht University
Princetonplein 1, 3584 CC, Utrecht (The Netherlands)
E-mail: m.e.leunissen@nyu.edu; a.vanblaaderen@uu.nl
[+] Present address: Center for Soft Matter Research, New York University, 4 Washington Place, New York, NY 10003 (USA)

DOI: 10.1002/adma.200900640

Interestingly, the relatively simple anisotropic dipolar interaction in a uniaxial field already gives rise to several new phases, like body-centered-tetragonal crystals.[9,20,21] Recently, Martin et al. reported for granular materials how *rotating* multi-axial fields can open up still another range of novel particle interactions.[11,22] They derived that in a rotating biaxial field the particles experience the following time-averaged interaction (here given for an electric field, neglecting higher-order multipole contributions; this is a reasonable approximation for the suspensions used in this report[20]):

$$U_{bi}(\mathbf{r}_{ij}) = -\frac{\pi\sigma^3\beta^2\varepsilon_m|\mathbf{E}|^2}{32}\left(\frac{\sigma}{r_{ij}}\right)^3\left(1-3\cos^2\theta_{ij}\right) \quad (1)$$

where σ is the particle diameter, $\boldsymbol{r}_{ij}$ the vector separating particles i and j, θ_{ij} the angle between $\boldsymbol{r}_{ij}$ and the normal to the plane of the rotating field, and the dielectric contrast factor $\beta = (\varepsilon_p - \varepsilon_m)/(\varepsilon_p + 2\varepsilon_m)$ with $\varepsilon_p/\varepsilon_m$ the dielectric constant of the particles/suspending medium at the frequency of interest.

Compared to the uniaxial field case, the particles in a biaxial field experience a negative dipolar interaction $\left(U_{bi} = -\frac{1}{2}U_{uni}\right)$. Computer simulations[13,23,24] and experiments with magnetizable particles[25,26] show that this modification of the sign of the dipolar interaction can lead to a macroscopically different suspension structure, with the particles separated into distinct layers. Microscopic information on (the evolution of) the three-dimensional particle configurations under the influence of the field is still missing, though. Also from a more general point of view, multi-axial fields have not yet received the attention that they deserve, especially not in light of their great potential for the generation of higher-complexity interactions[11,12] and new materials and technologies. Therefore, our goal is to establish a general, easy-to-use field application method and to explore in detail the control that multi-axial fields offer over colloidal suspensions, such that they can be used to actively direct the self-assembly of new structures. We use the inverted dipolar interaction in a biaxial field as our starting point, as this already leads to structures that are quite different from those seen in uniaxial fields. Moreover, to the best of our knowledge, an inverted dipolar interaction has not been demonstrated before for non-magnetic colloids (note that nearly all of the previous biaxial field work involved paramagnetic granular particles, which lack the ability to undergo free-energy driven self-organization).[22–25]

To create a generally applicable tool we use electric fields, because almost any material can be electrically polarized. Besides, magnetizable materials usually have a high density and absorb light strongly, making them less suitable for certain applications,

such as photonics, or to study by microscopy. Electric fields also offer other advantages: they are easy to generate, with thin electrodes instead of bulky Helmholtz coils, and the image dipoles in the electrodes reduce the depolarization field effect which complicates magnetic systems. To circumvent the problem of angular momentum transfer to the particles, as was observed for granular systems,[22] we did not use a truly rotating biaxial field but the equivalent of it, by applying a high-frequency 2D field vector with a randomized orientation. Here, we focus on the inverted dipolar interaction generated by a fully randomized biaxial field, but our method could also be easily extended to other interaction potentials by choosing different time-varying functions on the electrodes. The key feature is that we can switch the electronics very fast in comparison to the Brownian time scales of the suspension.

We constructed a sample cell with two mutually perpendicular pairs of semi-transparent electrodes (see Fig. 1a and the Experimental section), which allowed us to study the suspension structure in real time, by means of confocal microscopy. We calculated the electric field profile for a *yz* cross-section (Fig. 1b) and found that a region of at least $110 \times 110\ \mu m^2$ in the center of the cell should experience a nearly constant field strength ($E_{center} = 0.2325$–$0.2350\ V\mu m^{-1}$ for $\Delta V = 230$ V). Only the corners of the sample space suffer from a weak field gradient, $\vartheta(10^8)\ Vm^{-2}$, which induces slight dielectrophoretic effects in those areas[27] (Supporting Information, Fig. S1).

Figure 2 shows the ordered particle arrangements that resulted when we applied a biaxial field to a suspension of 2.00 μm PMMA-particles in density-matched CHB-decalin, with particle volume fraction $\varphi = 0.20$ and $\beta = -0.22$ ($\varepsilon_p < \varepsilon_m$). For moderate voltages, $\Delta V = 100$–120 V, we observed only a slight structuring of the initially isotropic suspension into short chains of particles, but at higher fields ($\Delta V = 140$–230 V) the particles assembled into 'sheet'-like structures of one particle thick, parallel to the (*yz*) plane of the field. In the *xy* cross-sections of Figure 2a the sheets appear as 'stripes', while the *yz* image of Figure 2-b4 show their internal structure. Importantly, each sheet consisted of multiple, differently oriented hexagonal domains, as there was no preferred orientation in the plane of the field. A clear orientational preference was only found close to the bottom/top wall, with one of the hexagonal close-packed directions running parallel to the wall (Figure 2-b4). This likely was a packing effect, but image charge interactions could play a role too.[21] Although our statistics on individual domains is somewhat limited, the internal ordering seems to be good, with a 2D hexagonal bond order parameter $\Psi_6 \approx 0.8$–0.9 for regions ranging in size from 45 to 70 μm on each side.

Besides the different domains, we observed a number of other defects. For instance, sheets often contained holes or had additional particles attached to their faces. Also, they could be truncated, or 'branched' instead. Although in the *xy* views of Figure 2a the sheets seem to be isolated structures, we found unexpected connections when we scanned through the sample cell, especially at intermediate fields ($\Delta V = 140$–180 V). Sometimes a part of one sheet was seen to bend over and get incorporated into a neighboring sheet, thus forming a 'bridge' between the two. We did not find such bridges at higher fields ($\Delta V = 230$ V), probably because the tilt out of the plane of the field is energetically unfavorable. Overall, our experimental structures compare well with computer simulation results.[13,23,24] It is important to note, however, that although the initial large-scale structuring of the suspension occurred within seconds, we found that it subsequently took many minutes for defects to anneal out, whereas the different hexagonal domains barely changed their orientation at all (Supporting Information, Movie S1 and S2).

The spacing between the sheets in our suspensions was quite regular. However, especially at high fields ($\Delta V = 230$ V) we found a distinct modulation, with neighboring sheets occasionally forming a tighter pair, although not always over their entire *y* extension (Figure 2a,b-1). When such a stacking occurred, the particle positions in the *xy* plane were seen to be shifted between the two sheets by half a particle diameter (along the *y* direction). This 'alternating' inter-sheet organization was clearest near the bottom (Figure 2b-2), due to the preferred lattice orientation imposed by the wall (deeper inside the bulk of the suspension the hexagonal domains of neighboring sheets have more often different orientations). Also in the perpendicular direction, shown in the *xz* image of Figure 2b-3, the sheets were seen to alternate.

It follows from the different confocal cross-sections that the paired sheets assumed an ABAB 'bridge-site' stacking; Figure 2c-1/2 shows a general example of this kind of stacking. This is remarkable, because from calculations of the dipolar interaction energy Martin et al. predicted a face-centered-cubic structure (fcc, Figure 2c-3),[13,23] which has a

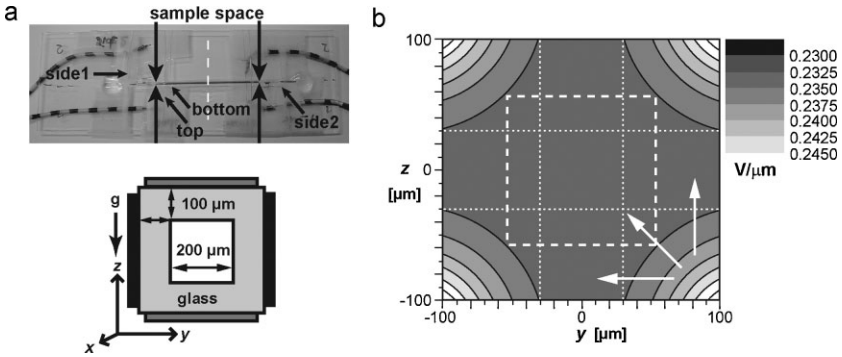

Figure 1. Biaxial electric field cell. a) Photograph and schematic drawing of the ~50 × 0.4 mm large sample cell, on top of a microscopy slide. Four wires provided independent contact to each of the plate electrodes, here indicated with small arrows. The large arrows indicate the length and width of the actual sample space and the dashed line indicates the cross-section that is schematically depicted below the photo. The two mutually perpendicular pairs of plate electrodes (of 12 nm thick) are indicated in dark grey and black. The plane of the electric field was parallel to the *yz* plane and the direction of gravity ('*g*'). b) Contour plot of the electric field profile in the *yz* plane for a total voltage difference $\Delta V = 230$ V between the two electrode pairs (the field strengths corresponding to other ΔV values can be found by linear scaling). Only the actual sample space of $200\ \mu m \times 200\ \mu m$ is shown. The dashed square highlights the central region with a nearly homogeneous electric field. The dotted lines demarcate the horizontal and vertical rectangular 'bands' with a nearly constant field strength all the way out to the bounding glass walls. The arrows indicate the expected direction of dielectrophoretic motion near the corners for a suspension with negative dielectric constant contrast ($\varepsilon_p < \varepsilon_m$).

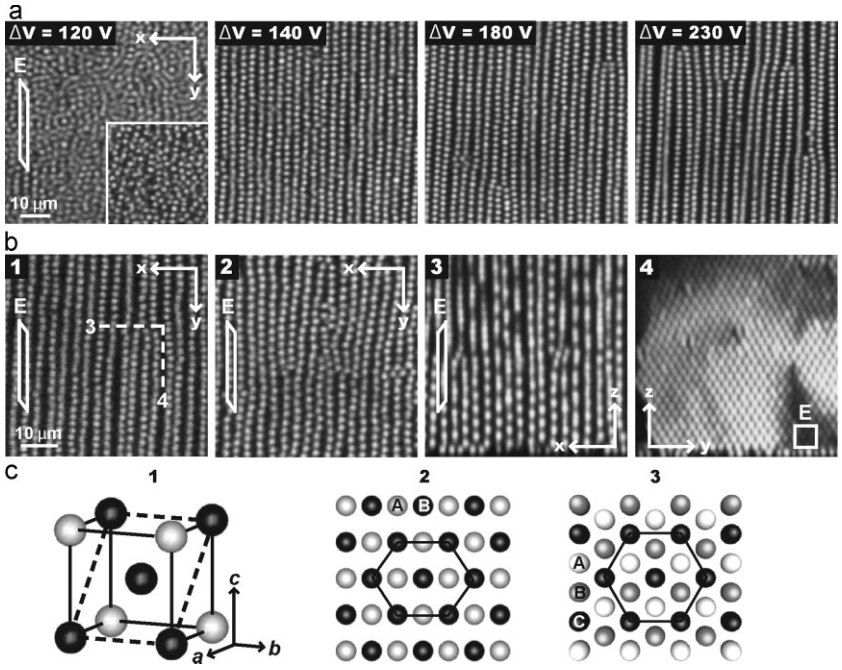

Figure 2. Suspension structure in a biaxial electric field. a) Confocal *xy* images of the center of the sample space (at height z = 0 and centered around y = 0 in Fig. 1b), 11 min after switching on different voltages. Each panel is the average of 10 frames, spanning 17 s in total. The inset at $\Delta V = 120$ V represents a single non-averaged snapshot to show how the Brownian motion of the particles caused the 'blurred' appearance of the averaged main panel, except where they formed larger, less-mobile structures. The skewed white rectangle indicates the orientation of the plane of the biaxial field 'E', perpendicular to the image. b) Differently oriented micrographs taken 11 minutes after switching on $\Delta V = 230$ V. (b-1): *xy* image of the center of the sample space ($z = 0$). The dashed lines indicate the orientations of images (b-3,4). (b-2): *xy* image, ~10 μm above the bottom wall of the sample space ($z = -90$ μm). (b-3): *xz* image immediately above the bottom wall at y = 0; the stretched appearance of the top part is a scanning artefact. (b-4): *yz* image immediately above the bottom wall halfway the length of the sample cell (the white square indicates the orientation of the plane of the biaxial field, parallel to the image). c) Model of a body-centered-cubic crystal structure, with $a = b = c$ (c-1). The spheres in subsequent (101) planes (dashed lines) are alternatingly colored black and white for ease of identification in the projection along the [101] direction (c-2), which reveals the ABAB bridge-site stacking of these nearly hexagonal layers. For comparison, (c-3) shows the ABC hollow-site stacking of the hexagonal (111) layers of a face-centered cubic structure (subsequent layers are colored white, grey and black).

'hollow-site' ABC stacking. We point out, though, that a stable bridge-site stacked structure has been observed before in the presence of a *uniaxial* electric field, namely in the form of body-centered-tetragonal (bct) crystals.[9,20,21,28] For simplicity, we have drawn a body-centered-cubic structure (bcc, $a = b = c$) in Figure 2c-1; the tetragonal structure only differs in that one axis is somewhat compressed ($a = b > c$, with the electric field parallel to the *c*-axis). If we forget about the exact lattice constants and only compare the qualitative characteristics of the body-centered model with our experimental observations (Figure 2b), we find that our hexagonal sheets in the *yz* plane correspond to the {101} planes of the model (both are bridge-site stacked), the *xz* cross-section to the {010} planes (seen under a 45° in-plane rotation) and the *xy* cross-section to the {10-1} planes. Despite its body-centered character the structure was neither bcc nor bct, though, because the bridge-site stacked sheets were spaced too far apart, except when they formed tight pairs like those seen at high fields. As far as we know, only Martin et al. have tried to determine what the most stable structure of a tight stack of multiple sheets in a biaxial field is.[13,23] Unfortunately, in their theory/simulations they did not consider structures other than fcc/hcp. Also note that the present structures, resulting from inverted dipolar interactions, are quite different from the structures that were found in computer simulations of layered ferrofluids[29], in which the particles have 'normal' dipolar interactions that were not induced by an external field. Five confined layers of such a ferrofluid were seen to form a bct-like structure, with the subsequent layers corresponding to the {100} planes.

Based on the above it seems probable that a compact, three-dimensional structure of stacked sheets is the thermodynamic ground state in a biaxial field. Nevertheless, we consistently ended up in a state of largely independent sheets, similar to the observed macroscopic structuring of granular and colloidal magnetic particles in a biaxial field.[25,26] From our experiments it appears that this is a non-equilibrium structure and that, in general, the suspension structure does not only depend on the configuration and strength of the field, but also on how the field is applied. Here, we applied the field instantaneously. This quickly led to many different hexagonal domains, which then connected up into larger sheets without changing their orientation much (Supporting Information, Movie S1 and S2). Obviously, neighboring sheets can only pair up into a larger three-dimensional structure if their domains have the same orientation. Also, when pairing up at a later stage, sheets need to temporarily bend out of the plane of the field, which carries a considerable energetic penalty. Note that at higher fields the inter-sheet interactions become more important, but that the energetic penalty for bending increases as well. A different field application strategy would likely lead to better sheets, with less different domains, and possibly a better developed three-dimensional structure. One could, for instance, ramp up the field more slowly, cycle it between high and low, or use a uniaxial 'pre-structuring' step into strings (see below) to induce a preferred orientation for the hexagonal domains.

Martin et al. have shown that the properties of biaxially structured materials, e.g. the electrical and thermal conductivities, can be strongly anisotropic.[13,23,25] The anisotropy is larger than for uniaxial fields and is 'spatially inverted', depending on the field configuration. In our sample cell we could easily apply a unixial field along one of the in-plane *y*/*z* directions; the resulting structure with 'strings' of particles parallel to the field lines is shown in Figure 3a. In Figure 3b and Supporting Movies S3–S4, we demonstrate how changing the field from zero to uniaxial to biaxial transformed the suspension structure within seconds from isotropic to one-dimensional strings and two-dimensional

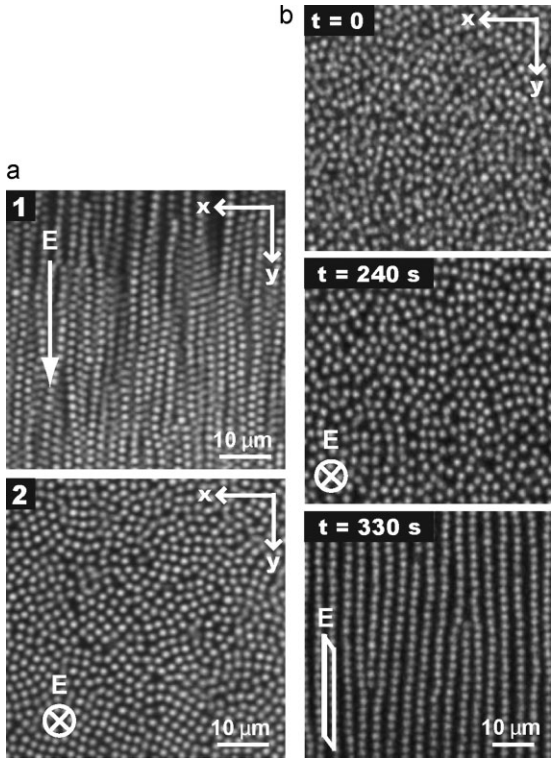

Figure 3. Switching between uniaxial and biaxial fields. a) Confocal *xy* images of the suspension structure in a uniaxial electric field ($\Delta V = 230$ V), taken after 11 minutes in the center of the sample space ($z = 0$). Each panel is the average of 10 frames, spanning 17 s in total. (a-1): Field along the *y* direction, between the pair of side electrodes. (a-2): Field along the *z* direction, between the pair of top and bottom electrodes. b, *xy* snapshots of the suspension structure in the center of the sample space ($z = 0$) during the switching sequence 'zero field – uniaxial field – biaxial field' ($\Delta V = 230$ V). The field was switched at $t = 10$ s (zero field → uniaxial) and $t = 250$ s (uniaxial → biaxial). The uniaxial field was oriented perpendicular to the imaging plane (i.e., along the *z* direction), giving the field-aligned strings at $t = 240$ s the appearance of individual particles just like in panel (a-2). Note, however, that their separation is larger than that of the truly single particles at zero field ($t = 0$). The skewed white rectangle at t = 330 s indicates the plane of the biaxial field, perpendicular to the image.

sheets. This could be useful for applications that require switchable, anisotropic material properties, like the viscosity or thermal conductivity. We point out, however, that it is also possible to permanently fix the field-structured material by suspending the particles in a suitable epoxy resin.[25,30] Moreover, we discovered that our polymer particles offer a surprisingly easy way to fix the individual particle structures as well (leaving the suspending medium liquid), namely by heating the sample for 1–2 minutes to 75–80 °C with the electric field on, using a stream of hot air that is much wider than the sample cell. This is followed by cooling through contact with the ambient air. We believe that at elevated temperature the steric stabilizer on the particle surface redistributes, so that particles that are in contact bind together. Upon cooling the particle stability is restored, and when we then switch off the (biaxial) field the result is a suspension of free-standing thin membranes, which can be dried and extracted from the capillary (Fig. 4 and Supporting Movie S5). Also if left in suspension, the structures are stable over time.

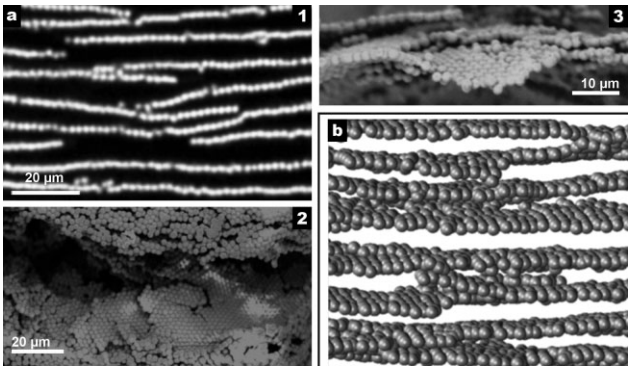

Figure 4. Self-supported permanent sheet structures after thermal annealing in a biaxial field ($\Delta V = 260$ V). a) Confocal microscopy scan of the permanent structures in solution (1) and electron microscopy scans (2-3) after removing the structures from the sample cell and drying them. The images are *xy* views of different parts of the sample and correspond to a top-bottom orientation of the long axis of the capillary that contained the suspension. b) Rendered particle coordinates revealing the three-dimensional structure of the permanent sheets (slightly tilted *xy* view). The particles are 2 μm in diameter.

In short, we have shown that electric fields offer a flexible way to manipulate colloidal interactions and their self-assembled structures and that this can be fruitfully extended beyond the previously studied uniaxial field case. That it is a generally applicable tool is confirmed by the observation that a biaxial electric field has the same effect on suspensions with a positive dielectric constant contrast ($\varepsilon_p > \varepsilon_m$, Supporting Fig. S2) as on the above described negative contrast suspensions ($\varepsilon_p < \varepsilon_m$). We have introduced an easy thermal annealing procedure to permanently fix the new structures and have demonstrated the good dynamic ('switching') control that multi-axial electric fields offer over the suspension structure. Both of these aspects should be interesting for applications, as the field-structured material properties can be strongly anisotropic. Furthermore, sample cells like the kind presented here allow us to obtain detailed information, on the single particle level, about the evolution of the suspension structure while the electric field is applied. This helps to identify the important factors in the colloidal self-assembly process and to optimize the final structures, as the latter seem to depend sensitively on how the field is applied. At the same time, one could continue to increase the complexity of the particle interactions. One can, for instance, easily obtain other interactions with our setup by choosing different time-varying functions on the electrodes. Also, with a triaxial field it might be possible to establish a colloidal model system with a Lennard–Jones-like interaction,[11] or one could combine the electric-field induced interactions with depletion or charge-mediated interactions. Besides, truly rotating fields could be used to obtain well-defined clusters of colloids,[11,12] which could then be turned into permanent molecule look-alikes with our thermal annealing procedure.

Experimental

Sample cell: We constructed a sample cell with two mutually perpendicular pairs of semi-transparent electrodes by sputter coating

the outer faces of a square borosilicate glass capillary (inner dimensions 0.2 mm × 0.2 mm and wall thickness 0.1 mm with a measured deviation of maximally 4 μm between different sides, $\varepsilon_g = 4.9$ at 1 MHz; Vitrocom) with 3 nm chromium and 9 nm gold (Cressington 208hr). Using a razor blade, we then removed the unwanted contact at the four corners of the square tubing. For the electrical contacts with each of the plate electrodes, we used silver paint and thin T2 thermocouple alloy wire (diameter 50 μm). The cell was constructed on top of a standard microscopy slide, for extra support.

Electric field generation: We used the equivalent of a rotating biaxial field, generated by applying a 2D electric field vector with a randomly varying orientation. To achieve this, we let an ordinary PC generate a random sequence of angles for the field vector, together with the corresponding voltage differences for the two electrode pairs. Typically, this pattern consisted of 10^4 steps (we did not observe any change in suspension behavior in the range of 10–10^6 steps). A NI 6534 Digital I/O card (16 Mb memory) was used to generate a digital representation of the correct voltage for each of the electrode pairs, while continuously repeating the random sequence with a frequency of 1 MHz ('pattern mode output'). Its output was converted by two 12 bits digital-to-analog converters (one for each of the electrode pairs) and then amplified to a maximum of 130 $V_{pk\text{-}pk}$ with an inverting and a non-inverting amplifier. The rise time of the amplification was 600 $V\mu s^{-1}$. We connected the two output channels with an oscilloscope to check the balancing of the field in a Lissajous plot of the amplitude. The overall field strength in the sample cell was set by the total voltage difference of the two electrode pairs. We determined the electric field profile inside the sample space with the freely available Poisson Superfish two-dimensional electrostatic field solver (Los Alamos National Laboratory). In our representation of the sample cell, we assumed the sample space to be filled with a solvent mixture of dielectric constant $\varepsilon_m = 5.8$ (see below).

Suspensions: We used suspensions of 2.00 μm, 2.04 μm and 3.9 μm diameter polymethylmethacrylate (PMMA) spheres ($\varepsilon_p \approx 2.6$ at 1 MHz), covalently labeled with the fluorescent dye 7-nitrobenzo-2-oxa-1,3-diazol and sterically stabilized with poly-12-hydroxystearic acid. We synthesized these particles by means of dispersion polymerization [31]. The size polydispersity was 3% for the ~2.0 μm particles and 5% for the 3.9 μm particles, as determined from light scattering and electron microscopy measurements. We suspended the 3.9 μm particles in as received *cis*-decalin ($\varepsilon_m = 2.2$) and the 2.00 μm particles in a mixture of this solvent (25% by weight) and as received cyclohexyl bromide (CHB), saturated with the salt tetrabutylammonium bromide (TBAB) to approach hard-sphere-like interactions. These solvents closely matched the refractive index of the particles, minimizing their van der Waals interactions (here, we take advantage of the fact that it is possible to match the polarizability of the particles and the solvent at optical frequencies, while maintaining a mismatch in dielectric properties at lower frequencies). The CHB–decalin mixture also nearly matched the particle density, preventing sedimentation during the experiment. We estimated the dielectric constant of the CHB-decalin mixture to be $\varepsilon_m = 5.8$, through correlation with the measured refractive indices of several mixtures and the pure CHB and *cis*-decalin solvents [32]. The PMMA particles were observed to selectively absorb a small fraction of the CHB from the mixture, which changed their effective density and dielectric constant (thereby changing their polarizability). Therefore, we let the suspension equilibrate for several days before filling the sample cell.

Confocal and electron microscopy: After filling the cell with the colloidal suspension, we sealed it with UV-curing optical adhesive (Norland no. 68), and studied it with confocal scanning laser microscopy (Leica NT CSLM). The orientation of the *xy*, *yz* and *xz* images with respect to the sample cell was as indicated by the coordinate system in Figure 1. For a more detailed investigation of the exact suspension structure we extracted the 3D particle coordinates from *xyz*-stacks, as it was described before by Royall et al. [33]. A single data stack consisted of 96 *xy* slices of 128 pixels × 128 pixels. The *xy* pixels were 200 nm × 200 nm in size, and the separation between the *xy* slices was 400 nm. After drying the sample, structures that were made permanent by thermal annealing were imaged with a FEI Phenom scanning electron microscope.

Acknowledgements

The authors would like to thank H. Wisman (Utrecht University, Soft Condensed Matter) for developing the electronics and control software needed for the electric-field generation, M.T. Sullivan (Princeton University) for providing the c script to generate the Poisson Superfish input files and G. Bosma (Utrecht University, Physical and Colloid Chemistry) and J.C.P. Stiefelhagen (Utrecht University, Soft Condensed Matter) for particle synthesis. This work was supported by the Stichting voor Fundamenteel Onderzoek der Materie and the Nederlandse Organisatie voor Wetenschappelijk Onderzoek. Supporting Information is available online from Wiley InterScience or from the authors.

Received: February 23, 2009
Revised: March 13, 2009
Published online: April 20, 2009

[1] V. J. Anderson, H. N. W. Lekkerkerker, *Nature* **2002**, *416*, 811.
[2] J. H. Holtz, S. A. Asher, *Nature* **2003**, *389*, 829.
[3] O. D. Velev, E. W. Kaler, *Adv. Mater.* **2000**, *12*, 531.
[4] J. J. Urban, D. V. Talapin, E. V. Shevchenko, C. R. Kagan, C. B. B. Murray, *Nat. Mater.* **2007**, *6*, 115.
[5] K. M. Ho, C. T. Chan, C. M. Soukoulis, *Phys. Rev. Lett.* **1990**, *65*, 3152.
[6] O. Sigmund, S. Torquato, *Appl. Phys. Lett.* **1996**, *69*, 3203.
[7] M. C. Rechtsman, F. H. Stillinger, S. Torquato, *Phys. Rev. Lett.* **2005**, *95*, 228301.
[8] A. van Blaaderen, *MRS Bulletin* **2004**, *29*, 85.
[9] A. Yethiraj, A. van Blaaderen, *Nature* **2003**, *421*, 513.
[10] K. Zahn, R. Lenke, G. Maret, *Phys. Rev. Lett.* **1999**, *82*, 2721.
[11] J. E. Martin, R. A. Anderson, R. L. Williamson, *J. Chem. Phys.* **2003**, *118*, 1557.
[12] G. Helgesen, A. T. Skjeltorp, *Physica A* **1991**, *170*, 488.
[13] J. E. Martin, R. A. Anderson, C. P. Tigges, *J. Chem. Phys.* **1999**, *110*, 4854.
[14] M. Parthasarathy, D. J. Klingenberg, *Mater. Sci. Eng. R.* **1996**, *17*, 57.
[15] J. Philip, P. D. Shima, B. Raj, *Applied Phys. Lett.* **2007**, *91*, 203108.
[16] W. B. Russel, D. A. Saville, W. R. Schowalter, *Colloidal Dispersions*, Cambridge University Press, Cambridge **1999**.
[17] V. N. Manoharan, M. T. Elsesser, D. J. Pine, *Science* **2003**, *301*, 483.
[18] S. C. Glotzer, *Science* **2004**, *306*, 419 and references herein.
[19] C. A. Mirkin, R. L. Letsinger, R. C. Mucic, J. J. Storhoff, *Nature* **1996**, *382*, 607.
[20] A.-P. Hynninen, M. Dijkstra, *Phys. Rev. E* **2005**, *72*, 051402.
[21] U. Dassanayake, S. Fraden, A. van Blaaderen, *J. Chem. Phys.* **2000**, *112*, 3851.
[22] T. C. Halsey, R. A. Anderson, J. E. Martin, *Int. J. Mod. Phys. B* **1996**, *10*, 3019.
[23] J. E. Martin, R. A. Anderson, C. P. Tigges, *J. Phys. Chem.* **1998**, *108*, 7887.
[24] S. Men, A. Meunier, C. Métayer, G. Bossis, *Int. J. Mod. Phys. B* **2002**, *16*, 2357.
[25] J. E. Martin, E. Venturini, J. Odinek, R. A. Anderson, *Phys. Rev. E* **2000**, *61*, 2818.
[26] P. Carletto, G. Bossis, A. Cebers, *Int. J. Mod. Phys. B* **2002**, *16*, 2279.
[27] H. A. Pohl, *Dielectrophoresis: The Behavior of Neutral Matter in Non-Uniform Electric Fields*, Cambridge University Press, Cambridge **1978**.
[28] R. Tao, J. M. Sun, *Phys. Rev. Lett.* **1991**, *67*, 398.
[29] R. A. Trasca, S. H. L. Klapp, *J. Chem. Phys.* **2008**, *129*, 084702.
[30] A. Yethiraj, J. H. J. Thijssen, A. Wouterse, A. van Blaaderen, *Adv. Mater.* **2004**, *16*, 596.
[31] G. Bosma, C. Pathmamanoharan, E. H. A. de Hoog, W. K. Kegel, A. van Blaaderen, H. N. W. Lekkerkerker, *J. Colloid Interf. Sci.* **2002**, *245*, 292.
[32] M. E. Leunissen, PhD thesis, Utrecht University, The Netherlands **2007**, available at www.colloid.nl.
[33] C. P. Royall, M. E. Leunissen, A. van Blaaderen, *J. Phys. Condens. Matter* **2003**, *15*, S3581.